Title
Enhancing glacier monitoring through adaptive smoothing of MODIS NDSI time series

Journal
Remote Sensing Letters, 15(10)

ISSN
2150-704X

Authors
Xin, Chen
Sheng, Yongwei

Publication Date
2024-10-02

DOI
10.1080/2150704x.2024.2398815

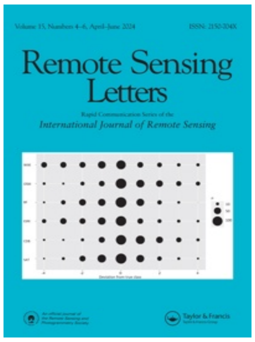

Remote Sensing Letters

ISSN: (Print) (Online) Journal homepage: www.tandfonline.com/journals/trsl20

Enhancing glacier monitoring through adaptive smoothing of MODIS NDSI time series

Chen Xin & Yongwei Sheng

REMOTE SENSING LETTERS
2024, VOL. 15, NO. 10, 1047–1056
https://doi.org/10.1080/2150704X.2024.2398815

Enhancing glacier monitoring through adaptive smoothing of MODIS NDSI time series

Chen Xin and Yongwei Sheng

Department of Geography, University of California-Los Angeles (UCLA), Los Angeles, CA, USA

ABSTRACT

Observation of glacier surface characteristics through remotely sensed time-series data is essential for understanding glacier seasonality, mass balance, and long-term trends. Yet, the reliability of these observations depends significantly on the quality of the time-series data. This study presents a meticulous preprocessing scheme to improve the quality of Moderate Resolution Imaging Spectroradiometer (MODIS) Normalized Difference Snow Index (NDSI) time-series data for glacier monitoring. We propose a three-step algorithm specifically crafted to overcome the challenges associated with cloud contamination reduction, outlier removal and data gap handling. This innovative approach iteratively compares the median values of automatically adjusted asymmetrical moving windows to achieve convergence, removing outliers using minimal window size to keep the temporal resolution as high as possible. The methodology's effectiveness is demonstrated through its application to two glaciers from the United States Geological Survey (USGS) Benchmark Project, showcasing significant improvements in the quality of smoothed MODIS NDSI time series. These results affirm the efficacy of the proposed scheme in rendering a more reliable evaluation of glacier surface condition and seasonal fluctuations. Consequently, this study contributes significant methodological advancements to the fields of remote sensing and glaciology, enhancing the accuracy of glacier monitoring techniques.

ARTICLE HISTORY
Received 12 April 2024
Accepted 25 August 2024

1. Introduction

Satellite remote sensing is a proven method for monitoring glacier status, offering detailed mapping of individual glaciers and identification of long-term trends (Gao and Liu 2001; Guo et al. 2015; Kaab et al. 2005; Konig, Winther, and Isaksson 2001; Paul et al. 2015). Typically, moderate-to-high spatial resolution products, such as the Landsat series and Sentinel-2, are utilized to capture snapshots of glacier properties. These snapshots facilitate the delineation of glacier boundaries (Pfeffer et al. 2014), monitoring of surface objects (Fahnestock et al. 2016; Paul et al. 2016), and classification of accumulation and ablation zones (Naegeli et al. 2017).

CONTACT Yongwei Sheng ysheng@geog.ucla.edu Department of Geography, University of California-Los Angeles (UCLA), Los Angeles, CA 90095-1524, USA

Supplemental data for this article can be accessed online at https://doi.org/10.1080/2150704X.2024.2398815

Beyond capturing static glacier characteristics, valuable insights can be gained from analysing glacier time series, which document the annual timing of critical events (e.g., the start and end of the ablation season) and long-term trends in glacier characteristics (Di Mauro and Fugazza 2022). To obtain time series that accurately reflect changes in glacier status, satellites offering frequent observations are essential. Over the last two decades, the MODIS (Moderate Resolution Imaging Spectroradiometer) instruments aboard the Aqua and Terra satellites have proven to be well-suited for this purpose, owing to their daily observational capabilities (Hall, Riggs, and Salomonson 1995). Consequently, MODIS daily time-series observations have become a cornerstone in the monitoring of seasonal snow cover and glacier seasonality (Di Mauro and Fugazza 2022; Muhammad and Thapa 2021).

To monitor glacier surface conditions, snow mapping algorithms for MODIS usually involve the derivation of the Normalized Difference Snow Index (NDSI) using Band 4 (0.545–0.565 μm) and Band 6 (1.628–1.652 μm), which effectively distinguish snow and ice signals (Hall et al. 2002). In addition to calculating NDSI, the generation of the MODIS Quality Assessment (QA) band flags the observation quality based on multiple spectral bands and observation geometry, thus facilitating the exclusion of cloud contaminations. While the QA band effectively masks clouds in most seasonal snow-related studies, using MODIS time-series data for alpine glacier research poses unique challenges, broadly falling into two categories: observation gaps and outliers. Extensive cloud masking often results in consecutive observation gaps due to prevalent cloud cover. Additionally, residual clouds, debris, and terrain shadows can significantly alter satellite observation, leading to outliers in the NDSI time series (Hall and Riggs 2007; Klein and Barnett 2003; Paul et al. 2016).

Preprocessing algorithms have been developed in response to these issues. To improve binary snow map accuracy, Gafurov and Bárdossy (2009) introduced a comprehensive six-step workflow to enhance binary snow map accuracy, with key strategies including the amalgamation of Aqua and Terra daily observations, leveraging adjacent day observations and neighbouring pixels and incorporating snow transition elevation data. Similarly, Dong and Menzel (2016) also merged Aqua and Terra data and applied neighbouring pixel analysis, integrating precipitation and temperature filters to reduce misclassification between snow and cloud. Di Mauro and Fugazza (2022) addressed gaps and outliers in time-series observation by excluding outliers deviating more than 2 standard deviations from the median within an 11-day kernel, filling gaps through linear interpolation and applying a Fast Fourier Transform (FFT) low-pass filter (99-day kernel) for smoothing. Nevertheless, these approaches present certain drawbacks. For instance, using linear interpolation to fill gaps could be rather erroneous, especially when outliers are not properly removed beforehand. Moreover, the moving window technique faces challenges in selecting a fixed window size. Small windows may fail to effectively eliminate outliers, while large windows risk over-smoothing the data. Additionally, adjusting window sizes demands a nuanced understanding of each study area's distinct features, suggesting a need for a self-adaptive approach suitable for applications across more extensive regions.

To address these challenges, this study proposes an iterative moving median filter for MODIS NDSI time-series observations, which is a robust and adaptive processing strategy. The general workflow employs a variable moving window that automatically increases its

Table 1. Two USGS Benchmark glaciers used in this study.

RGI ID	Glacier Name	Area (km^2)	Slope (°)	Aspect (°)	Longitude (°W)	Latitude (°N)
RGI60-02.17023	Sperry Glacier	1.28	18.9	345	113.76	48.62
RGI60-02.18778	South Cascade Glacier	2.92	12.8	350	121.06	48.36

size asymmetrically to remove outliers and fill gaps simultaneously. This approach accounts for various sized gaps with the asymmetric moving window, offering a more reasonable moving median calculation. By gradually enlarging the moving window, we ensure that closer observations are prioritized, therefore minimizing temporal offsets. Furthermore, by iteratively applying this asymmetrical moving window until the median stabilizes, we eliminate the need for location-specific fixed window size, rendering our method self-adaptive to various locations and climatic conditions. The effectiveness of this workflow was demonstrated on selected USGS Benchmark glaciers, highlighting its potential for accurate seasonal glacier ice variation monitoring.

2. Study site and dataset used

This study validates the proposed processing strategy using glacier sites from the USGS Benchmark Glacier Project (henceforth, the Benchmark Project) (O'Neel et al. 2019). Two mid-latitude glaciers selected are South Cascade Glacier, in a maritime climate, and Sperry Glacier, in a continental climate. Table 1 shows the key characteristics of these glaciers as of the year 2000 according to Randolph Glacier Inventory (RGI) Version 6.0 (Pfeffer et al. 2014). Due to space limitations, a map showing the location of these glaciers is included in the supplementary material.

In this study, the MODIS MOD10A1.061 product (Terra Snow Cover Daily Global 500 m) NDSI measurement is utilized to monitor snow and ice signals from 2001 to 2022 (Hall et al. 2002). Though previous studies have leveraged Terra MODIS, Aqua MODIS, or both to investigate snow and ice, the Aqua product is not used in this study due to its failure in Band 6 sensor. This sensor failure affects the shortwave infrared (SWIR) measurements, which are crucial for consistent NDSI calculation (Di Mauro and Fugazza 2022; Muhammad and Thapa 2021). The data retrieval process is expedited by utilizing the Google Earth Engine (GEE) platform (Gorelick et al. 2017), allowing efficient access to NDSI time series for our selected study sites. We extracted per-pixel NDSI values and binary cloud masks for each glacier. RGI 6.0 provides the glacier boundaries, reflecting their status in the year 2000 (Pfeffer et al. 2014).

Figure 1 displays the original pixel-based NDSI time series of the study glaciers for the year 2013, climatically a normal year (NOAA/NCEI 2014). Both glaciers exhibit a scattered time series with substantial cloud contamination and outliers, with a noticeable dip in the summer season. Thus, it is essential to preprocess the time series by screening clouds and outliers before identifying any temporal patterns.

3. Method

The proposed time series processing workflow is structured into three steps. The first step employs the QA band to mitigate cloud contamination, which effectively reduces the

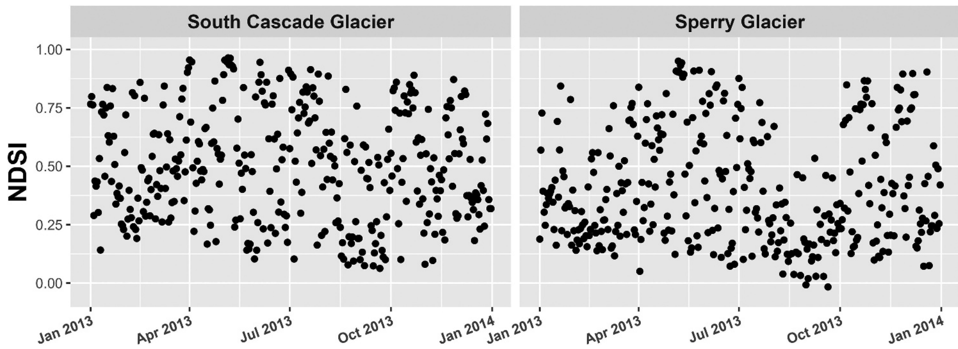

Figure 1. Raw 2013 MODIS NDSI time series for the South Cascade and Sperry glacier.

presence of clouds but leaves behind observation gaps and outliers from other sources. To mitigate these issues, the second step employs an innovative moving median algorithm iteratively. This iterative moving median filter not only removes outliers using the smallest possible window but also fills in gaps with the calculated median. The final step involves the application of an FFT low-pass filter to the outlier-removed time series to capture the seasonal patterns within the NDSI time series by mitigating high-frequency natural variations. An overview of this workflow is shown as a flowchart in Figure 2.

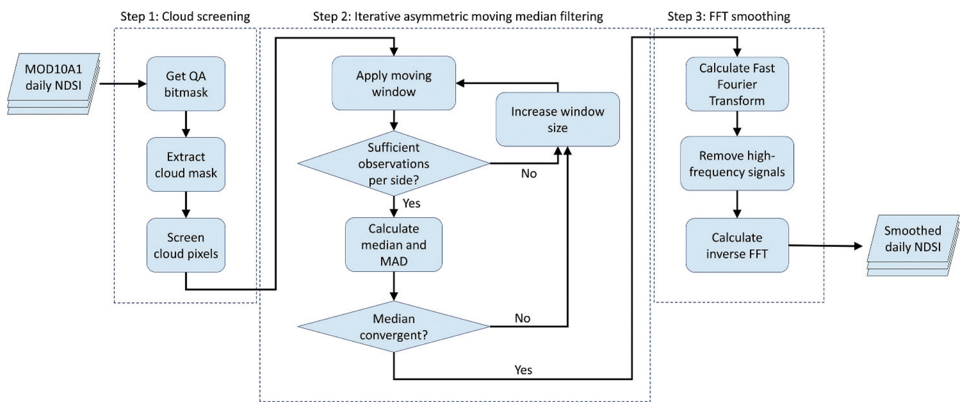

Figure 2. Flowchart of the smoothing algorithm workflow.

3.1. Cloud screening

The first step begins by generating daily binary cloud masks using the MOD10A1 product's QA band. These masks are applied to the NDSI images to facilitate the export of per-pixel daily time series. Per-pixel extraction excludes cloud-covered pixels from that day's observation, ensuring only clear-sky observations contribute to the dataset, thus enhancing data utilization efficiency.

Figure 3 illustrates the cloud screening results for the two glaciers with substantial low observation points (grey dots) removed. Despite the strong screening capability, a significant portion of observations are cloud-covered—73.7% for Sperry Glacier and

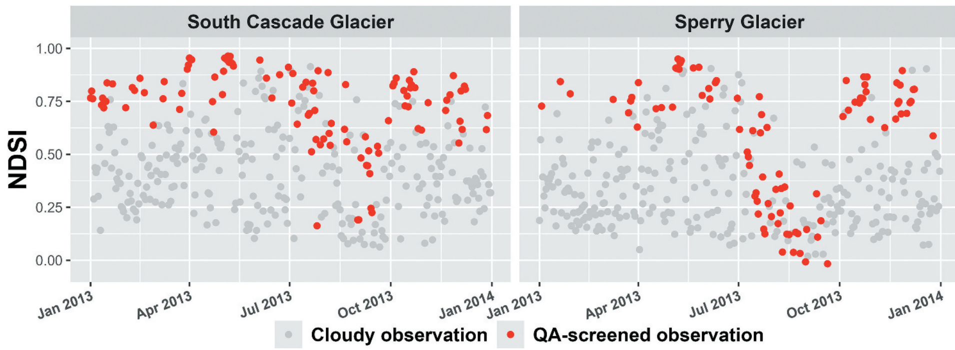

Figure 3. NDSI time series for the South Cascade and Sperry Glacier after QA cloud screening. Gray dots represent cloudy observations; red dots represent QA-screened observations.

71.2% for South Cascade Glacier – resulting in large gaps in the time series. Both glaciers have a comparable number of gaps and average gap sizes (Sperry Glacier: 49 gaps, 5.5 days average; South Cascade Glacier: 51 gaps, 5.1 days average). However, Sperry Glacier has a larger maximum gap size of 38 days compared to South Cascade Glacier's 23 days. In addition to the induced gaps, the remaining cloud-free observations are still scattered with significant variability, suggesting the presence of remaining outliers that will need to be addressed in subsequent processing steps.

3.2. *Iterative asymmetrical moving median filtering*

After screening out dense cloud contamination, the NDSI time series contains consecutive gaps and still exhibits remarkable outliers due to residual clouds and terrain influences. To tackle these challenges, we propose an Iterative Asymmetrical Moving Median Filter (IAMMF), inspired by Sheng et al. (1995) in their vegetation time series preprocessing work, which dynamically adjusts the moving window size until convergence is achieved. Our process starts with the smallest 3-day window, gradually expanding to include additional valid observations on either side, guided by a 'valid observation threshold' (notated as '*n*'). Additionally, the design of the asymmetrical window enables rapid enlargement towards the side with larger gaps, effectively minimizing the overall window size and reducing the over-smoothing issue.

Following the first iteration, which attains more than one valid observation per side, the algorithm calculates the median alongside the median absolute deviation (MAD) using the valid observations within the moving window. Further iterations continue, each designed to incorporate '$n + 1$' valid observations on both sides for a balanced valid data distribution in the window, until a stable median is achieved. Median stability is evaluated by comparing the change in median to a predefined threshold, e.g., half of the MAD from the preceding smaller window. To avoid excessive expansion, the algorithm restricts the larger window side to no more than twice the length of the shorter side, with the shorter side limited to a maximum of 30 days.

Figure 4 illustrates how the algorithm filters outliners and bridges a gap in the original time series at a certain day (i.e., Day 0). Starting with a 3-day window, the first iteration yields one valid observation on each side, producing a median of 58.5 and a MAD of 2.22.

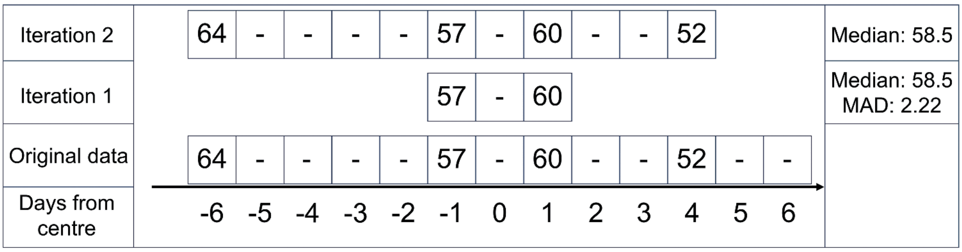

Figure 4. An example showing IAMMF filtering procedure.

As the window extends and eventually includes four valid observations within Day −6 and Day +4, the recalculated median remains at 58.5. Given the median change is zero, confirming 58.5 as the smoothed value for that day.

3.3. *Time series smoothing for seasonality extraction*

After removing outliers and filling gaps, we apply a Fast Fourier Transform (FFT) low-pass filter to accentuate long-term seasonality. This method attenuates fluctuations with periods shorter than approximately 40 days by keeping only the lowest 5% frequency signals from a daily series over a year. Choosing this 5% threshold over a lower one allows us to track seasonality without overly smoothing the data. This choice is also advantageous because the preceding IAMMF effectively mitigates outliers, making it safer to maintain higher frequency signals, which in turn enhances the accuracy of the smoothed NDSI time series.

4. Results

The effectiveness of the proposed algorithm is showcased by analysing the 2013 annual NDSI time series for both Sperry Glacier and South Cascade Glacier. Figure 5 illustrates a comparison between Mauro and Fugazza's method Figure 5(a) and the IAMMF algorithm Figure 5(b), highlighting the distinct approaches to managing outliers and gaps. Mauro and Fugazza's method uses an 11-day moving median for outlier removal (red dots) followed by linear interpolation for gap filling (blue dots). In contrast, IAMMF combines outlier removal and gap filling with values from a stable moving median, ensuring a more consistent NDSI time series. Figure 5(a) shows scattered patterns with outlier contamination and variable zigzags due to linear interpolation. IAMMF Figure 5(b) produces a smoother time series, effectively removing outliers and filling gaps. The adaptability of IAMMF further enhances its capacity to accommodate characteristics of different glaciers. Notably, despite the time series at South Cascade Glacier is noisier compared to Sperry Glacier, particularly in August, IAMMF consistently delivers filtered values without a noticeable increase in local variance.

Moving window filtering theoretically improves time-series data quality by sacrificing temporal resolution. IAMMF uses the smallest possible window to minimize this sacrifice. We define 'temporal offset' as the positional difference between the median value and the window target point to quantify the sacrifice of temporal resolution, with a smaller value

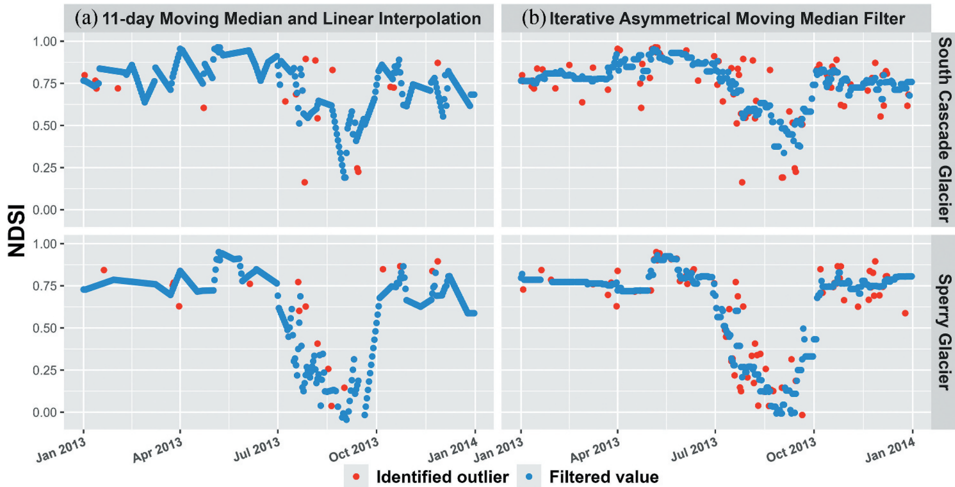

Figure 5. NDSI time series for the South Cascade and Sperry Glacier after further filtering. Red dots represent outliers; blue dots represent filtered values by using Mauro and Fugazza approach (a) or IAMMF (b).

indicating minimal sacrifice in the smoothed time series. Consequently, we delve into analysing the temporal offset distributions produced by the IAMMF for both study glaciers, as depicted in Figure 6. Specifically, the average temporal offset is 9.7 days for Sperry Glacier and 7.5 days for South Cascade Glacier. A mere 9% of observations for Sperry Glacier and 6.5% for South Cascade Glacier exhibit a temporal offset exceeding 20 days, primarily due to substantial gaps within the NDSI time series.

With the gaps filled and most outliers corrected in the preceding steps, the NDSI data refined by the IAMMF is then fed into a 5% threshold FFT low-pass filter to capture seasonal patterns. The 5% FFT threshold proficiently reduces variations in the NDSI time series with periods shorter than 40 days. Figure 7 compares the FFT performance on both Mauro and Fugazza's and IAMMF filtered time series. The IAMMF, by creating a more smoothed time series compared to the method by Mauro and Fugazza, enables the FFT filter based on the IAMMF results to more accurately delineate NDSI seasonality. This accuracy is particularly noticeable in the

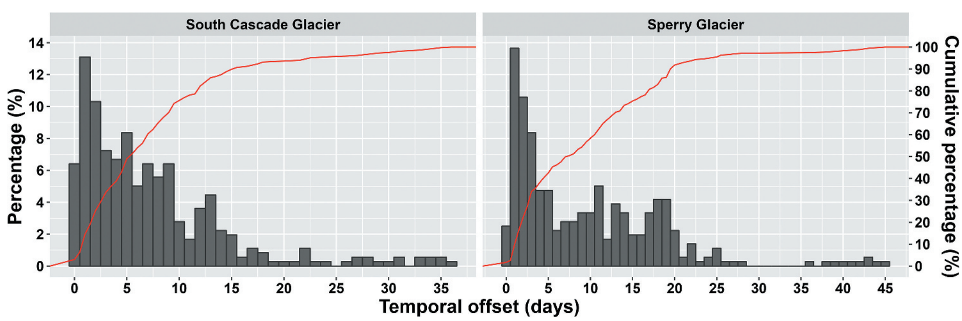

Figure 6. Histograms showing temporal offset distribution for the South Cascade and Sperry Glacier. Corresponding cumulative percentage is shown in red curve.

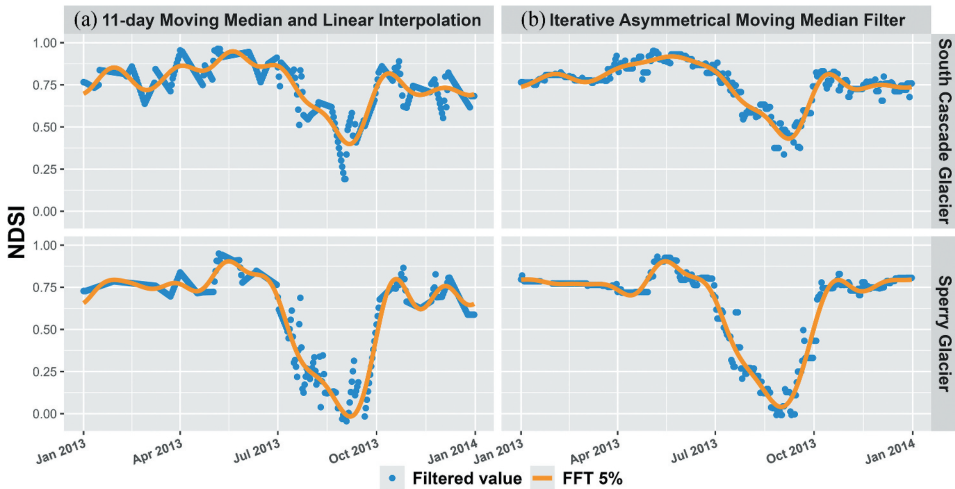

Figure 7. FFT smoothed NDSI time series for the South Cascade and Sperry Glacier. After filtering NDSI by Mauro and Fugazza approach (a) or IAMMF (b), blue dots are the primary FFT input. Orange curve is smoothed output of the FFT low-pass filter using 5% threshold.

analysis of Mauro and Fugazza's results for Sperry Glacier from November to December, where their FFT smoothed time series erroneously reflects a zig-zag pattern. This pattern is an artefact of their linear interpolation method for gap filling, highlighting the advantages of the IAMMF approach in producing a more reliable seasonal representation.

To assess the effectiveness of the 5% FFT smoothing, we calculated the Root Mean Square Error (RMSE) between the FFT-smoothed NDSI series and the filtered, gap-free time-series data. The analysis reveals a notable decrease in RMSE for both study glaciers when applying the IAMMF compared to Mauro and Fugazza's approach. Specifically, the RMSE for Sperry Glacier reduced from 0.064 to 0.043, and for South Cascade Glacier, it dropped from 0.06 to 0.036, roughly a > 30% drop in both cases. These reductions in RMSE demonstrate a closer alignment of the FFT smoothing with the IAMMF-filtered values, thus underscoring the IAMMF's superior capability in enhancing the accuracy of FFT-smoothed NDSI time-series data.

5. Conclusion

In this research, we have developed and implemented an innovative processing scheme for MODIS NDSI time series glacier monitoring. This three-step workflow can efficiently remove outliers, fill data gaps, and smooth the data to accentuate NDSI seasonality. The proposed approach employs a variable moving window that automatically increases its size asymmetrically to remove outliers and fill gaps simultaneously. This approach accounts for various sized gaps with the asymmetric moving window, offering a more reasonable moving median calculation. By iteratively gradually enlarging the moving window, the innovative filter ensures that closer observations are prioritized, therefore minimizing temporal resolution sacrifice.

The algorithm's efficacy was demonstrated through its application to two glaciers from the Benchmark Project. Our results validate the effectiveness of our processing strategy and demonstrate its advantages over conventional methods, underscoring its contribution to advancing glacier monitoring practices. The proposed strategy improves the quality of NDSI time series for glacier monitoring and facilitates more reliable evaluations of glacier surface condition and seasonal changes.

To move forward, we plan to apply the proposed preprocessing techniques to refine albedo and fractional snow cover area (fSCA) time series and use good-quality time series to investigate glacier phenology. Moreover, the integration of high spatial and temporal resolution datasets from Landsat 8, Landsat 9 and Sentinel-2 presents the potential for more detailed glacier phenology analyses, leveraging the strengths of multiple remote sensing platforms for enhanced accuracy in glaciological studies.

Disclosure statement

No potential conflict of interest was reported by the author(s).

ORCID

Chen Xin http://orcid.org/0000-0001-6103-1108

Data availability statement

MODIS NDSI data can be accessed through Google Earth Engine: https://developers.google.com/earth-engine/datasets/catalog/MODIS_061_MOD10A1.

References

Di Mauro, B., and D. Fugazza. 2022. "Pan-Alpine Glacier Phenology Reveals Lowering Albedo and Increase in Ablation Season Length." *Remote Sensing of Environment* 279. https://doi.org/10.1016/j.rse.2022.113119.

Dong, C. Y., and L. Menzel. 2016. "Improving the Accuracy of MODIS 8-Day Snow Products with in situ Temperature and Precipitation Data." *Journal of Hydrology* 534:466–477. https://doi.org/10.1016/j.jhydrol.2015.12.065.

Fahnestock, M., T. Scambos, T. Moon, A. Gardner, T. Haran, and M. Klinger. 2016. "Rapid Large-Area Mapping of Ice Flow Using Landsat 8." *Remote Sensing of Environment* 185:84–94. https://doi.org/10.1016/j.rse.2015.11.023.

Gafurov, A., and A. Bárdossy. 2009. "Cloud Removal Methodology from MODIS Snow Cover Product." *Hydrology and Earth System Sciences* 13 (7): 1361–1373. https://doi.org/10.5194/hess-13-1361-2009.

Gao, J., and Y. S. Liu. 2001. "Applications of Remote Sensing, GIS and GPS in Glaciology: A Review." *Progress in Physical Geography-Earth and Environment* 25 (4): 520–540. https://doi.org/10.1177/030913330102500404.

Gorelick, N., M. Hancher, M. Dixon, S. Ilyushchenko, D. Thau, and R. Moore. 2017. "Google Earth Engine: Planetary-Scale Geospatial Analysis for Everyone." *Remote Sensing of Environment* 202:18–27. https://doi.org/10.1016/j.rse.2017.06.031.

Guo, W. Q., S. Y. Liu, L. Xu, L. Z. Wu, D. H. Shangguan, X. J. Yao, J. F. Wei, et al. 2015. "The Second Chinese Glacier Inventory: Data, Methods and Results." *Journal of Glaciology* 61 (226): 357–372. https://doi.org/10.3189/2015JoG14J209.

Hall, D. K., and G. A. Riggs. 2007. "Accuracy Assessment of the MODIS Snow Products." *Hydrological Processes* 21 (12): 1534–1547. https://doi.org/10.1002/hyp.6715.

Hall, D. K., G. A. Riggs, and V. V. Salomonson. 1995. "Development of Methods for Mapping Global Snow Cover Using Moderate Resolution Imaging Spectroradiometer Data." *Remote Sensing of Environment* 54 (2): 127–140. https://doi.org/10.1016/0034-4257(95)00137-P.

Hall, D. K., G. A. Riggs, V. V. Salomonson, N. E. DiGirolamo, and K. J. Bayr. 2002. "MODIS Snow-Cover Products." *Remote Sensing of Environment* 83 (1–2): 181–194. https://doi.org/10.1016/S0034-4257(02)00095-0.

Kaab, A., C. Huggel, L. Fischer, S. Guex, F. Paul, I. Roer, N. Salzmann, et al. 2005. "Remote Sensing of Glacier- and Permafrost-Related Hazards in High Mountains: An Overview." *Natural Hazards and Earth System Sciences* 5 (4): 527–554. https://doi.org/10.5194/nhess-5-527-2005.

Klein, A. G., and A. C. Barnett. 2003. "Validation of Daily MODIS Snow Cover Maps of the Upper Rio Grande River Basin for the 2000-2001 Snow Year." *Remote Sensing of Environment* 86 (2): 162–176. https://doi.org/10.1016/S0034-4257(03)00097-X.

Konig, M., J. G. Winther, and E. Isaksson. 2001. "Measuring Snow and Glacier Ice Properties from Satellite." *Reviews of Geophysics* 39 (1): 1–27. https://doi.org/10.1029/1999rg000076.

Muhammad, S., and A. Thapa. 2021. "Daily Terra-Aqua MODIS Cloud-Free Snow and Randolph Glacier Inventory 6.0 Combined Product (M*D10A1GL06) for High-Mountain Asia Between 2002 and 2019." *Earth System Science Data* 13 (2): 767–776. https://doi.org/10.5194/essd-13-767-2021 .

Naegeli, K., A. Damm, M. Huss, H. Wulf, M. Schaepman, and M. Hoelzle. 2017. "Cross-Comparison of Albedo Products for Glacier Surfaces Derived from Airborne and Satellite (Sentinel-2 and Landsat 8) Optical Data." *Remote Sensing* 9 (2). https://doi.org/10.3390/rs9020110.

NOAA/NCEI. 2014. "Monthly Drought Report for Annual 2013." https://www.ncei.noaa.gov/access/monitoring/monthly-report/drought/201313.

O'Neel, S., C. McNeill, L. C. Sass, C. Florentine, E. H. Baker, E. Peitzsch, D. McGrath, A. G. Fountain, and D. Fagre. 2019. "Reanalysis of the US Geological Survey Benchmark Glaciers: Long-Term Insight into Climate Forcing of Glacier Mass Balance." *Journal of Glaciology* 65 (253): 850–866. https://doi.org/10.1017/jog.2019.66.

Paul, F., T. Bolch, A. Kaab, T. Nagler, C. Nuth, K. Scharrer, A. Shepherd, et al. 2015. "The Glaciers Climate Change Initiative: Methods for Creating Glacier Area, Elevation Change and Velocity Products." *Remote Sensing of Environment* 162:408–426. https://doi.org/10.1016/j.rse.2013.07.043.

Paul, F., S. H. Winsvold, A. Kaab, T. Nagler, and G. Schwaizer. 2016. "Glacier Remote Sensing Using Sentinel-2. Part II: Mapping Glacier Extents and Surface Facies, and Comparison to Landsat 8." *Remote Sensing* 8 (7). https://doi.org/10.3390/rs8070575.

Pfeffer, W. T., A. A. Arendt, A. Bliss, T. Bolch, J. G. Cogley, A. S. Gardner, J. O. Hagen, et al. 2014. "The Randolph Glacier Inventory: A Globally Complete Inventory of Glaciers." *Journal of Glaciology* 60 (221): 537–552. https://doi.org/10.3189/2014JoG13J176.

Sheng, Y. W., W. Y. Chen, Q. G. Xiao, and L. A. Guo. 1995. "Macro Classification of Vegetation in China with NOAA/NDVIs." *Chinese Science Bulletin* 40 (10): 839–844.